Applied and Computational Mathematics
2018; 7(1-2): 1-11
http://www.sciencepublishinggroup.com/j/acm
doi: 10.11648/j.acm.s.2018070102.11
ISSN: 2328-5605 (Print); ISSN: 2328-5613 (Online)

Bifurcation Behaviour and Stability Analysis of a Nano-Beam Subjected to Electrostatic Pressure

Aydin Azizi[1], Niloofar Malekzadeh Fard[2], Hamed Mobki[3], Adnène Arbi[4, 5, *]

[1]Department of Engineering, German University of Technology, Muscat, Oman

[2]Department of Biomedical Engineering, Islamic Azad University, Science and Research Branch, Tehran, Iran

[3]Department of Mechanical Engineering, University of Tabriz, Tabriz, Iran

[4]Higher Institute of Applied Sciences and Technology of Kairouan, Department of Mathematics Physics and Computer Science, University of Kairouan, Kairouan, Tunisia

[5]Laboratory of Engineering Mathematics, Tunisia Polytechnic School, University of Carthage, Tunis, Tunisia

Email address:

Aydin.Azizi@gutech.edu.om (A. Azizi), niloofar.malekzadeh@yahoo.com (N. M. Fard), hamedmobki@live.com (H. Mobki), adnen.arbi@gmail.com (A. Arbi)

[*]Corresponding author

To cite this article:

Aydin Azizi, Niloofar Malekzadeh Fard, Hamed Mobki, Adnène Arbi. Bifurcation Behaviour and Stability Analysis of a Nano-Beam Subjected to Electrostatic Pressure. *Applied and Computational Mathematics.* Special Issue: Recurrent neural networks, Bifurcation Analysis and Control Theory of Complex Systems. Vol. 7, No. 1-2, 2018, pp. 1-11. doi: 10.11648/j.acm.s.2018070102.11

Received: June 16, 2017; **Accepted**: June 19, 2017; **Published**: July 11, 2017

Abstract: This paper deals with the study of bifurcation behavior of a capacitive nano-beam considering electrostatic, Casimir and van der Waals forces. A modified mass-spring model has been implemented for analysis of the nano-beam behavior. The model has been adjusted and corrected with Euler-Bernoulli beam model, because of its less accuracy compared to distributed models. Fixed or equilibrium points of the nano-beam have been obtained, and has been shown that with variation of the applied voltage and the length of the nano-beam as control parameters the number of equilibrium points is changed. The stability of the fixed points has been investigated drawing motion trajectories in phase portraits and basins of attractions and repulsion have been illustrated. Critical values of the applied voltage and the length of the nano-beam leading to qualitative changes in the nano-beam behavior have been obtained.

Keywords: Nano-Beam, Electrostatic Force, Van der Waals Force, Casimir, Stability

1. Introduction

With the fast growth of nano scale technology, the possibility of substituting this new technology with micro technology, due to high speed and low energy consuming has been increased. NEM devices such as, nano-tweezers [1-2], super sensitive sensor [3-4], resonators [5], electrostatic switches [6-7], random access memory [8], vapor and strain sensors [9] are widely designed, analyzed, fabricated and used.

Electrostatically actuated devices form a broad class of MEMS and NEMS devices due to their simplicity, as they require few mechanical components and small voltage levels for actuation [10]. In such devices, a conductive flexible beam/plate is suspended over a ground plate and a potential difference is applied between them. As the micro/nanostructure is balanced between electrostatic attractive force and mechanical (elastic) restoring force, both electrostatic and elastic restoring force are increased when the electrostatic voltage increases. When the voltage reaches the critical value, pull-in instability occurs. Pull-in is a situation at which the elastic restoring force can no longer balance the electrostatic force. Further increase of the voltage will cause the structure to have dramatic displacement jump, resulting in structural collapse and failure. Pull-in instability is a snap-through like behavior and it is saddle-node bifurcation type of instability [11].

In NEM systems, by decreasing the geometric dimension, Casimir and van der Waals (vdW) effects play a major role, especially, in terms of the mechanical behavior of these

systems. More than five decades ago, Hendrik Brugt Gerhard Casimir (1909–2000) predicts that the ground-state energy of photons is alternated in the presence of two parallel perfectly conducting metal plates in such a way as to lead to an observable macroscopic force between them [12-13]. His brief article discusses the discovery, formulation, physical significance, and impact of one of the phenomena that bears his name, the eponymous Casimir effect [13]. The vdW force is related to the electrostatic interaction between dipoles at the atomic scale [14]. One of the most important differences between these two forces is that the Casimir force between plates depends only on the spacial properties of the objects whereas the vdW force depends on both the material properties as well as the geometric properties [15].

The pull-in phenomenon is widely applied in many micro/nano-machined devices that require bi-stability for their operation, such as NEM switches [16]. Many studies have been concentrated in the analysis of statitcal as well as dynamical stability of micro structures [17-20]. In nano scale, Dequesnes et al [6] have studied the Pull-in phenomena and pull-in voltage of a carbon-based nano-electromechanical switch. Fathi and Muhammad investigated chaotic behavior of a curved carbon nanotube under harmonic excitation [21]. Vakili-Tahami et al [15] have studied static and dynamic pull-in phenomenon of capacitive nano-beam, using Euler-Bernoulli beam model. Lin and Zhao [13, 16, and 22] have researched static and dynamic behavior of nano-beam and presented new parameter for detachment length and showed that there are two equilibrium points in extremity. In other paper [23], they have studied stability and bifurcation behavior of electrostatic torsional NEM varactor and also they used mass-spring model for their researches.

In spite of many research accomplished on the stability of MEMS and NEMS structures, there is not enough comprehensive study explaining their stability from bifurcation view point. Therefore, in order to show the equilibrium positions of a NEMS structure and their stability, this paper as a case study considers a nano-beam suspended over a conductive plate actuated by an electrostatic force applying a DC polarization voltage. The nonlinear equation of dynamic motion of the Euler–Bernoulli nano-beam using a one term Galerkin weighted residual method is replaced by a lumped mass-spring model. Due to the low accuracy of this model in studying of static and dynamic behavior of the nano-beam in comparison with the distributed model, the mass-spring model is attuned with beam one to increase its accuracy using corrective coefficients. Equilibrium position or fixed points is identified by solving equation of static deflection, and is illustrated in the state-control space. Furthermore, motion trajectories of nano-beam are drawn in phase portraits.

2. Model Description

Figures 1. a and 1. b show schematic views of a NEM switch and its cross-section, respectively. It consists of a nano-beam suspended over a stationary conductor plate, with length L, thickness h, width b, and initial gap of G_0. The nano-beam is considered isotropic with Young modulus E, density ρ and cross section moment of inertia I.

Attractive electrostatic force due to an applied voltage as well as vdW and Casimir forces pulls the nano-beam down towards the substrate. The minimum length of the nano-beam in which vdW and Casimir forces lead the nano-beam to collapse on the substrate (in lack of the electrostatic force), is known as the detachment length.

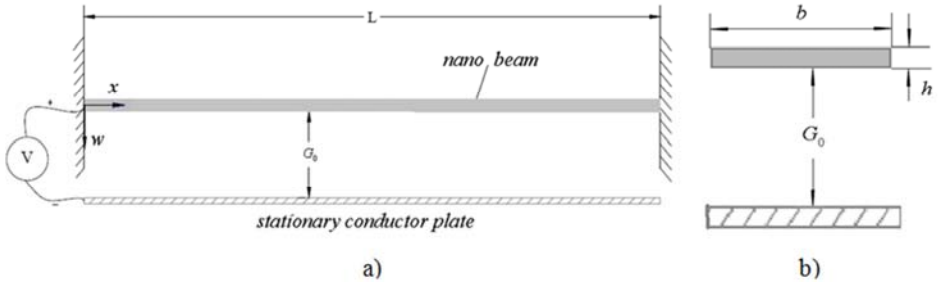

Figure 1. *Schematic view of a beam-based NEM switch: a) A beam-based NEM switch, b) Cross section of the nano beam.*

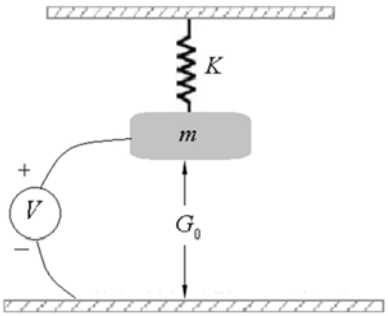

Figure 2. *Mass-spring model of nano-beam.*

In order to simplify the analysis of bifurcation behavior of the nano beam, the model shown in Figure 1 is substituted by a mass-spring model, which is shown in Figure 2. In the next section the mathematical model of the nano beam based on mass-spring assumption and its adjustments with the Euler-Bernolli beam model will be presented.

3. Mathematical Modeling and Solution

Considering a continuum based Euler-Bernoulli beam theory, governing equation for dynamic motion of a capacitive nano-beam taking into account vdW and Casimir forces with

distributed parameters can be obtained as following [24]:

$$EI\frac{\partial^4\hat{w}}{\partial\hat{x}^4}+\rho S\frac{\partial^2\hat{w}}{\partial\hat{t}^2}=q_{ext} \tag{1}$$

where $\hat{w}(x,t)$ *is* the transversal deflection of the nano-beam, S is the cross section area of the nano-beam and q_{ext} is the sum of electrostatic, vdW and Casimir forces, so:

$$q_{ext}=q_{elect}+q_{vdW}+q_{Casimir} \tag{2}$$

When the actuating voltage is applied between the nano-beam and substrate, the electrostatic force per unit length is computed using a standard parallel capacitance model [25] and is equal with:

$$q_{elect}=\frac{\varepsilon_0 bV^2}{2(G_0-\hat{w})^2} \tag{3}$$

and the vdW force per unit length of the nano-beam is given by [26]:

$$q_{vdW}=\frac{Ab}{6\pi(G_0-\hat{w})^3} \tag{4}$$

Also, Casimir force between nano beam and substrate is given by [12]:

$$q_{caimir}=\frac{b\pi^2\hbar c}{240(G_0-\hat{w})^4} \tag{5}$$

in equations (3)-(5) $\varepsilon_0=8.854\times10^{-12}C^2N^{-1}m^{-2}$ is the permittivity of vacuum within the gap, V is the electrical potential difference applied to the beam and substrate, G_0 is the initial gap between the beam and substrate, and $A=\pi^2C\rho_1^2$ is Hamaker constant, which lies in the range of $(0.4-4)\times10^{-19}J$ [27], $\hbar=1.055\times10^{-34}J.s$ is the Planck's constant and $c=2.998\times10^8 ms^{-1}$ is the speed of light.

In order to compose a lumped mass-spring model for the nano-beam, "Eq. (1)" is replace by "Eq. (6)" [16]

$$m\frac{d^2\hat{y}}{d\hat{t}^2}+K\hat{y}=\frac{\varepsilon_0 bLV^2}{2(G_0-\hat{y})^2}+\frac{AbL}{6\pi(G_0-\hat{y})^3}+\frac{b\pi^2\hbar cL}{240(G_0-\hat{y})^4} \tag{6}$$

where m is the mass of the nano-beam and equals to ρSL, K is the equivalent elasticity stiffness of the nano-beam which for fixed-fixed and cantilever nano-beam are equal to $\frac{384EI}{L^3}$ and $\frac{8EI}{L^3}$, respectively, and $\hat{y}(t)$ is the deflection of mass in the lumped model [16].

In order to enhance the accuracy of the mass-spring model and adjusting this model with the distributed model, equivalent mass as well as corrective coefficients of, a_0, b_0 and c_0 are applied as:

$$m_{eq}\frac{d^2\hat{y}}{d\hat{t}^2}+K\hat{y}=a_0\left[\frac{\varepsilon_0 bLV^2}{2(G_0-\hat{y})^2}\right]+b_0\left[\frac{AbL}{6\pi(G_0-\hat{y})^3}\right]+c_0\left[\frac{b\pi^2\hbar cL}{240(G_0-w)^4}\right] \tag{7}$$

where m_{eq} is the equivalent mass of the nano-beam, and a_0 (electrostatic corrective coefficient), b_0 (vdW corrective coefficient), and c_0 (Casimir corrective coefficient) are determined from equating of the first natural frequency, static pull-in voltage and detachment length of the mass-spring with those obtained using distributed model, respectively.

For convenience "Eq. (1)" and "Eq. (7)" can be rewritten in a non-dimensional form using the following non-dimensional parameters:

$$w=\frac{\hat{w}}{G_0},\ y=\frac{\hat{y}}{G_0},\ x=\frac{\hat{x}}{L},\ t=\frac{\hat{t}}{t*} \tag{8}$$

where $t*$ for the mass-spring and Euler-Bernoulli beam model equals to $\sqrt{\frac{m_{eq}}{K}}$ and $\sqrt{\frac{\rho SL^4}{EI}}$, respectively. Therefore "Eq. (1)" and "Eq. (7)" can be changed as:

$$\frac{\partial^2 w}{\partial t^2}+\frac{\partial^4 w}{\partial x^4}=\frac{\alpha' V^2}{(1-w)^2}+\frac{\beta'}{(1-w)^3}+\frac{\gamma'}{(1-w)^4} \tag{9}$$

$$\frac{d^2 y}{dt^2}+y=\frac{\alpha V^2}{(1-y)^2}+\frac{\beta}{(1-y)^3}+\frac{\gamma}{(1-y)^4} \tag{10}$$

where β and β' are non-dimensional parameters of the vdW force, γ and γ' are non-dimensional parameters of the Casimir force and α and α' are the non-dimensional parameters of the electrostatic force in the mass-spring and distributed model, respectively. These parameters are:

$$\beta'=\frac{AbL^4}{6\pi EIG_0^4},\ \beta=\frac{b_0 AbL}{6\pi KG_0^4}$$

$$\gamma'=\frac{b\pi^2\hbar cL^4}{240EIG_0^5},\ \gamma=\frac{c_0 b\pi^2\hbar cL}{240KG_0^5}$$

$$\alpha'=\frac{\varepsilon_0 bL^4}{2EIG_0^3},\ \alpha=\frac{a_0\varepsilon_0 bL}{2KG_0^3} \tag{11}$$

The governing equation for the static deflection of the Euler-Bernoulli nano-beam using "Eq. (9)" is given as:

$$\frac{d^4 w}{dx^4}=\frac{\alpha' V^2}{(1-w)^2}+\frac{\beta'}{(1-w)^3}+\frac{\gamma'}{(1-w)^4} \tag{12}$$

4. Results and Discussion

4.1. Determination of Corrective Coefficients

The natural frequency of the corrective mass-spring and

the distributed model (in the absence of electrostatic, vdW, and Casimir forces) are computed and equalized to the each other. So equivalent mass of the nano-beam for the fixed-fixed and cantilever beam can be obtained respectively, as:

$$m'_{cantilever} = 0.65m\,,\ m'_{fixed-fixed} = 0.74m \tag{13}$$

The values of pull-in voltage and detachment parameters for the mass-spring and the distributed model are obtained using SSLM and Galerkin based reduced order model [15, 24]. In order to obtain coefficient b_0, c_0 and a_0, detachment parameters and pull-in voltage of the distributed and the mass-spring model are equalized to each other. These parameters for cantilever and fixed-fixed nano-beam are:

$$b_0^{cantilever} = 0.68\,,\ b_0^{fixed-fixed} = 0.79$$

$$c_0^{cantilever} = 0.69\,,\ c_0^{fixed-fixed} = 0.8$$

$$a_0^{cantilever} = 0.71\,,\ a_0^{fixed-fixed} = 0.82 \tag{14}$$

4.2. Bifurcation Analysis Without Imposing Electrostatic Force

This section deals with equilibrium points of nano-beam considering vdW and Casimir forces. With attention to dimensionless Eq. (10), physically equilibrium or fixed points exist in the range of $0 < y < 1$. However, mathematically, these points may also exist in the range of $y > 1$. By setting $w = \dot{y}$, Eq. (10) can be transformed into the following form:

$$\frac{dy}{dt} = w$$

$$\frac{dw}{dt} = \frac{\alpha V^2}{(1-y)^2} + \frac{\beta}{(1-y)^3} + \frac{\gamma}{(1-y)^4} - y \tag{15}$$

At the equilibrium points, the nano-beam is at rest, hence considering Eq. (15), equilibrium points are obtained by the following equation:

$$w = 0$$

$$\frac{\alpha V^2}{(1-y)^2} + \frac{\beta}{(1-y)^3} + \frac{\gamma}{(1-y)^4} - y = 0 \tag{16}$$

For obtaining of fixed points without the electrostatic force, following equation must be solved by setting $V = 0$.

$$f(\alpha,\beta,\gamma,V,y) = \alpha V^2(1-y)^2 + \beta(1-y) + \gamma - y(1-y)^4 = 0 \tag{17}$$

The order of algebraic Eq. (17); is five with respect to y, having at most three real roots. Positions of the fixed points in the state-control space versus detachment parameters as a control parameter; β are illustrated in Figure 3.

In order to check stability in the vicinity of each equilibrium point, the following Jacobian matrix is used [16].

$$J = \begin{bmatrix} 0 & 1 \\ \dfrac{2\alpha V^2}{(1-y)^3} + \dfrac{3\beta}{(1-y)^4} + \dfrac{4\gamma}{(1-y)^5} - 1 & 0 \end{bmatrix} \tag{18}$$

with eigenvalues of the Jacobean satisfies in $\lambda^2 - (\frac{2\alpha V^2}{(1-y)^3} + \frac{\beta}{(1-y)^4} + \frac{\gamma}{(1-y)^5} - 1) = 0$ so $\lambda^2 = \frac{2\alpha V^2}{(1-y)^3} + \frac{\beta}{(1-y)^4} + \frac{\gamma}{(1-y)^5} - 1$. For $\lambda^2 < 0$, it has two pure imaginary roots, which means that the equilibrium point (y_1, β_1) is a center point. Applying the same method to the other equilibrium point (y_2, β_1), its eigenvalues satisfy $\lambda^2 > 0$, indicating two real eigenvalues, one is positive, and the other is negative. This means that the equilibrium point is an unstable saddle point [16]. Using this method, the stability in the vicinity of each equilibrium point in Figure 3 can be identified. In this paper, continuous and dashed curves represent stable and unstable branches, for state control spaces, respectively.

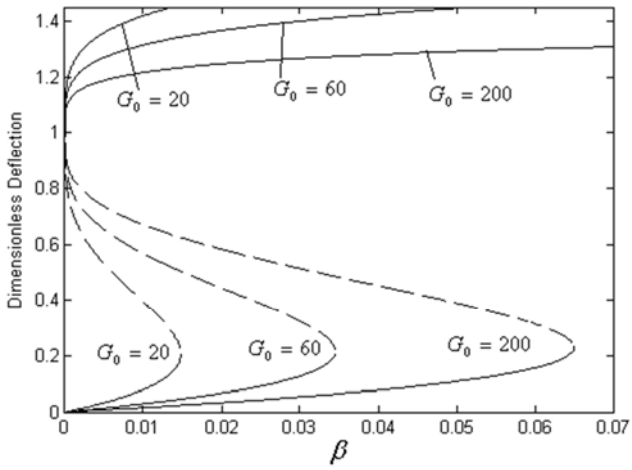

Figure 3. *Equilibrium points of a static nonlinear model as β is varied.*

As shown in Figure 3 for a given β there exist at most three fixed points. Based on the illustrated motion trajectories in phase portraits, the first and third fixed point is a stable center and the second one is an unstable saddle node.

As shown in Figure 3, by increasing the control parameter β, two physically fixed points are getting close together. For example for $G_0 = 60nm$ in $\beta = 0.035$, which is called as detachment length in NEMS literatures, they meet together in a saddle node bifurcation point. Figs. 4-7 present motion trajectories of the nano-beam for different values of β for $G_0 = 60nm$ with different initial values.

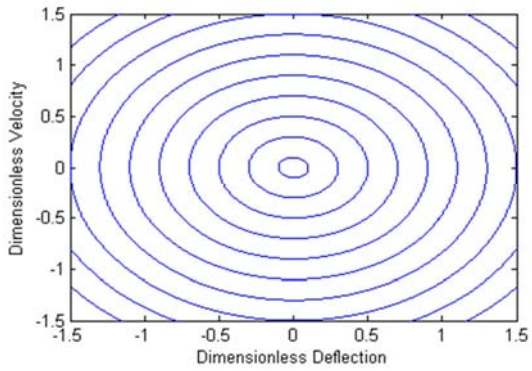

Figure 4. *Phase diagram with given* $\beta = 0$.

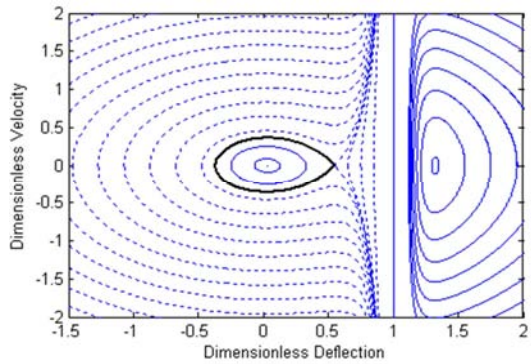

Figure 5. *Phase diagram with given* $\beta = 0.01$.

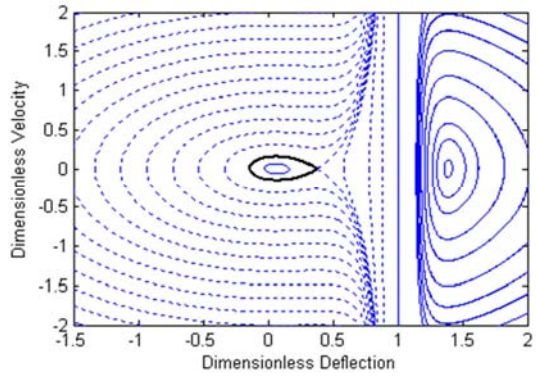

Figure 6. *Phase diagram with given* $\beta = 0.02$.

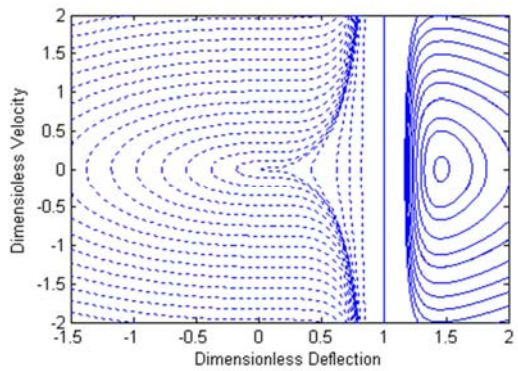

Figure 7. *Phase diagram with given* $\beta = 0.035$.

As shown in Figs. 5-6 there are a basin of attraction of stable centers and a region of repulsion of unstable saddle node. Of course, it must be noted that the substrate position acts as a singular point and velocity of the system near this singular point tends to infinity. The basin of attraction of the first stable center is bounded by a closed orbit. Depending on the location of the initial condition, the system can be stable or unstable. Figures 5-7 show that with increasing the parameter β the basin of attraction of stable centre is contracted; and when β equals to the detachment parameter, there is no physically basin of attraction and the system will be unstable for any initial condition. In this paper, continues, dashed and bold curves represent, periodic, unstable and Homoclinic trajectories for the phase portraits, respectively.

Figs. 8 and 9 show equilibrium points versus β and γ, which either vdW or Casimir force considered, respectively.

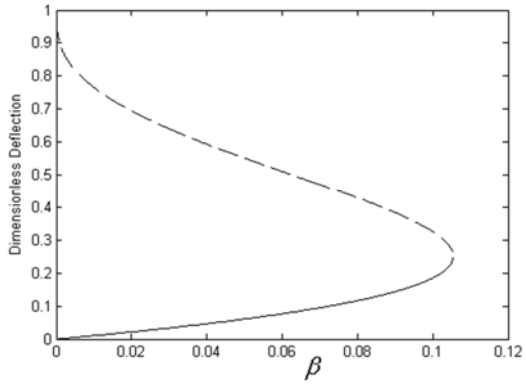

Figure 8. *Equilibrium points of a static nonlinear model as* β *is varied for* $\gamma = 0$.

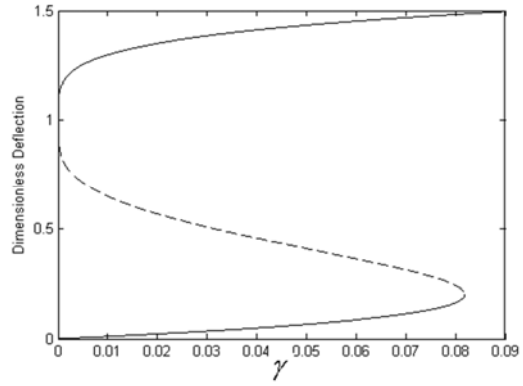

Figure 9 *Equilibrium points of a static nonlinear model as* γ *is varied for* $\beta = 0$

As shown in Figure 8 and 9 for $\beta < 0.106$ and $\gamma < 0.082$ there exist two and three fixed points, respectively. Based on Jacobian matrix (Eq. (18)) the first fixed point is a stable center and the second one is an unstable saddle. The third fixed point in the case of $\beta = 0$ is stable center.

By increasing the control parameter β and γ two physically fixed points are becoming close together and for $\beta = 0.106$ and $\gamma = 0.082$, which is called as detachment parameter in the NEMS literatures, they meet eachother in a

saddle node bifurcation point. Figs. 10 and 11 present motion trajectories of the nano-beam for given different parameter of β and γ.

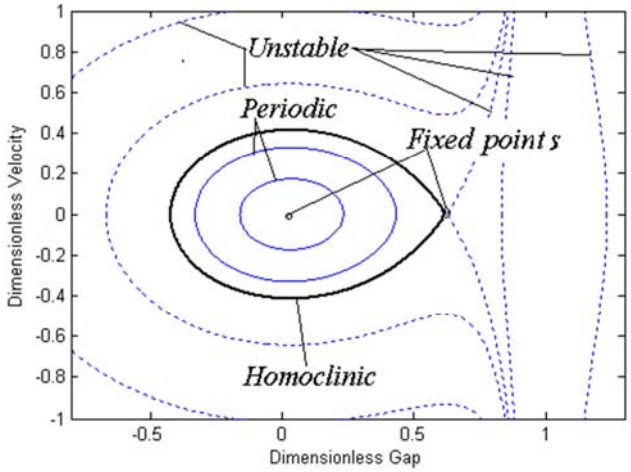

Figure 10. *phase diagram with given* $\beta = 0.03$ *and* $\gamma = 0$.

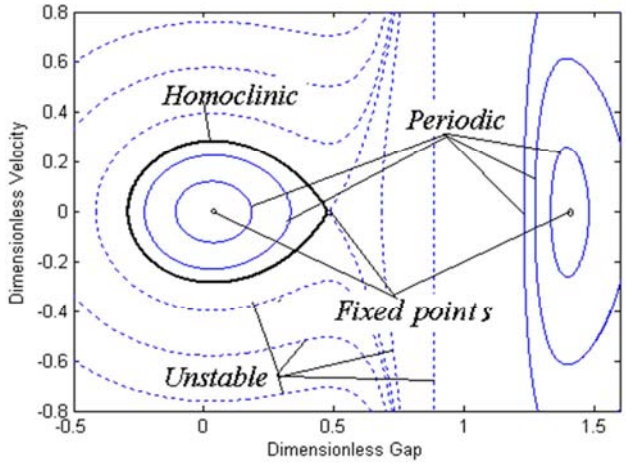

Figure 11. *phase diagram with given* $\gamma = 0.03$ *and* $\beta = 0$.

4.3. Bifurcation Analysis with Considering VDW, Casimir and Electrostatic Forces

Fixed points of the nano-beam in the presence of the electrostatic force and considering vdW and Casimir forces can be obtained by solving Eq (17). Order of algebraic "Eq. (17)" is five, with respect to *y*, and the number of pure real roots depends on the value of applied voltage. Figure 12 depicts equilibrium points for a nano-beam versus applied voltage as a control parameter. The cantilever nano-beam properties are *L=500nm, h=20nm, b=50nm, E=169GPa* and $G_0 = 60nm$. The stability in the vicinity of each fixed point can be recognized with the mentioned procedure and using Jacobin matrix, presented in Eq. (18). As shown in Figure 12 for $V < 12.11 = V_{pull-in}$ there are three fixed points and for $V > 12.11 = V_{pull-in}$ there excists only one fixed point.

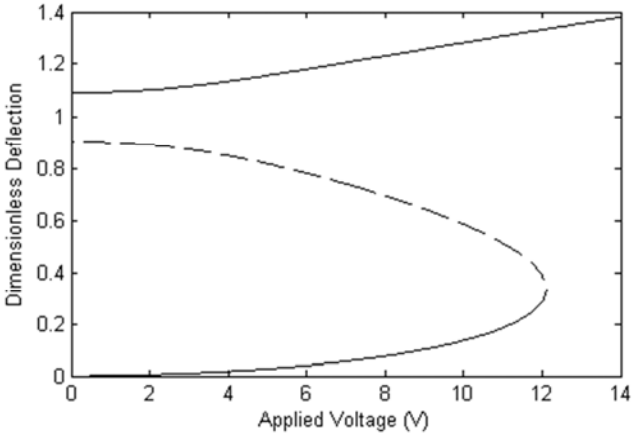

Figure 12. *Equilibrium points of a static nonlinear model as* V *is varied.*

Figs. 13-16 show phase diagrams of the nano-beam in the presence of electrostatic force with different applied voltages. As shown in these figures there exist center and saddle type fixed points. Figures 13-15 show that by increasing the applied voltage, the basin of attraction of stable centre is contracted and when V=12.11V which known as pull-in voltage in MEMS and NEMS literatures there is no physically basin of attraction and the system is unstable for every initial condition. This scenario represents saddle node bifurcation.

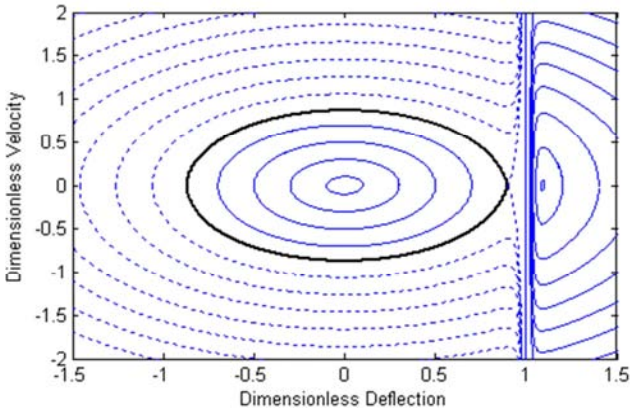

Figure 13. *Phase diagram with given* $V = 0$.

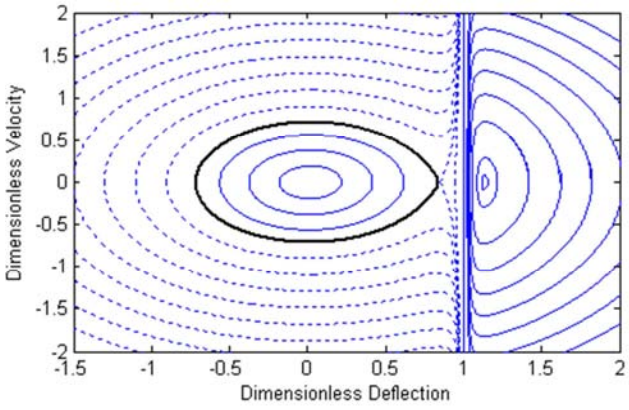

Figure 14. *Phase diagram with given* $V = 4$.

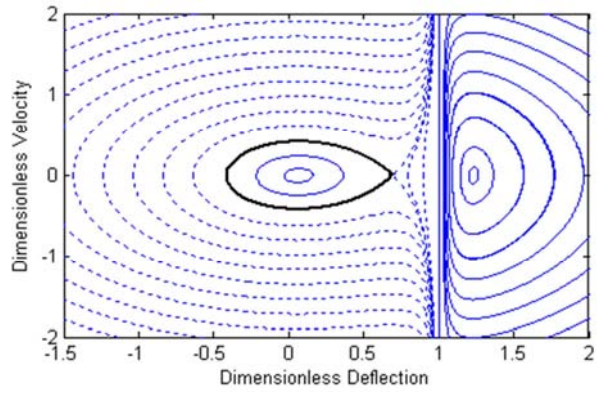

Figure 15. *Phase diagram with given* $V = 8$.

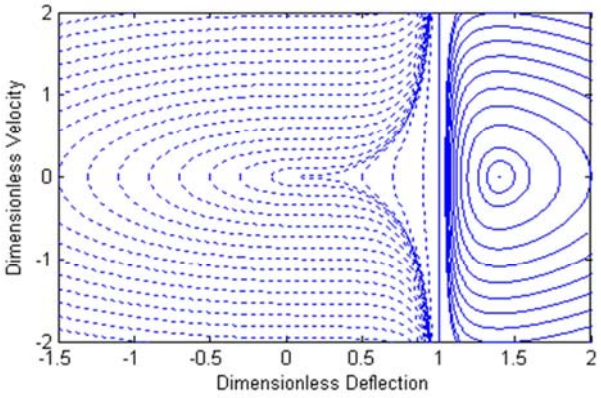

Figure 16. *Phase diagram with given* $V = V_{pull-in} = 12.11$.

In the following by neglecting the Casimir force (i.e. considering vdW force with imposing electrostatic force), the bifurcation behavior of a nano-beam is investigated. As will be shown, by neglecting this force, some new phenomena come out, which have not been addressed before.

Figs. 17-19 depict equilibrium points for nano-beams versus applied voltage as a control parameter. Fixed-fixed nano-beams properties are *b=10nm, h=3nm,* $G_0 = 4nm$, and the length of the each nano-beam is written in the related figures. Increasing the length of nano-beams causes to increase the effects of vdW forces, but decreases the pull-in voltage [15]. For example as shown in Figs. 17-19 when the length of nano-beams is equal to *65nm* and *80nm*, two equilibrium points in each voltage range of $0 < V < 2.92$ and $0 < V < 2.68$ appear. Also, in the range of $2.92 < V < V_{pull-in}$ and $2.68 < V < V_{pull-in}$ respectively, four equilibrium points are produced, where the third and fourth fixed points are physically impossible because of its location in the beneath of the substrate. However, there are only two equilibrium points in voltage range $0 < V < V_{pull-in}$ for the nano-beam with length of *100nm*. For the mentioned nano-beams by increasing the control parameter V the physically possible fixed points are getting close together and in the pull-in voltage, they emerge as a saddle node bifurcation point.

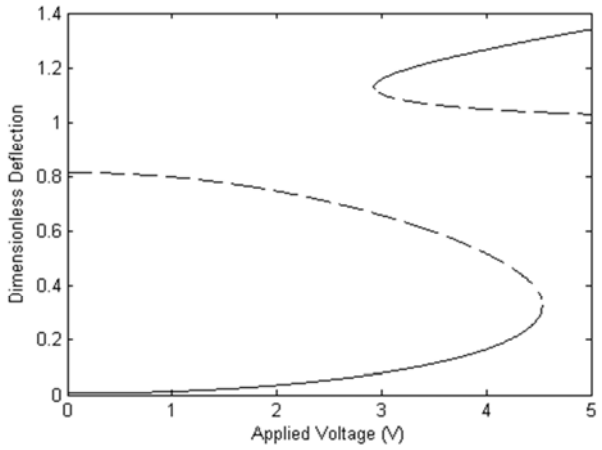

Figure 17. *Variation of equilibrium points with length 65nm.*

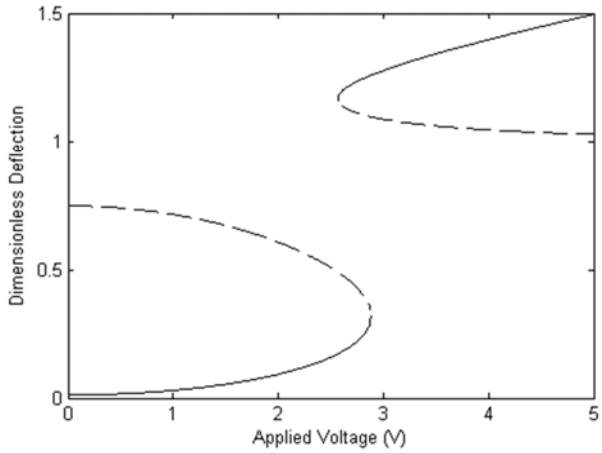

Figure 18. *Variation of equilibrium points with length 80nm.*

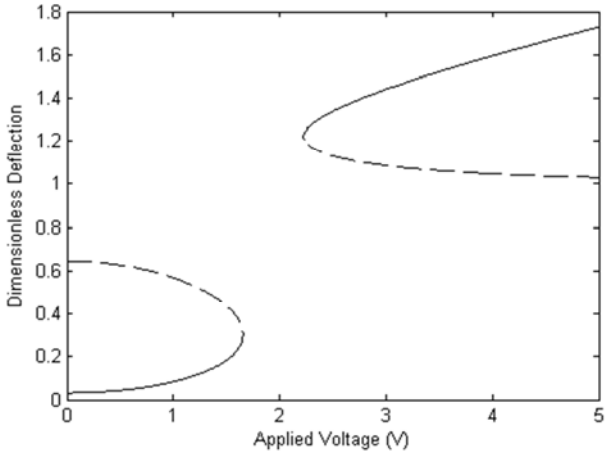

Figure 19. *Variation of equilibrium points with length 100nm.*

In Figs. 20-24 the phase diagram of the nano-beam with length of *65nm* are presented. As shown there exist a center and a saddle type fixed points in the range of $0 < y < 1$ with the voltage range $0 < V < 2.92$. By increasing the applied voltage, these points getting closer to each other, and it is observed that, another saddle and center fixed points in $y > 1$ in voltage range of $V > 2.92$ appear. With increasing applied voltage, these fixed points move away from each other. In

$V = 2.92v$ and $V = V_{pull-in}$ saddle and center points located in the upper side of the substrate coalesces and the basin of attraction disappears.

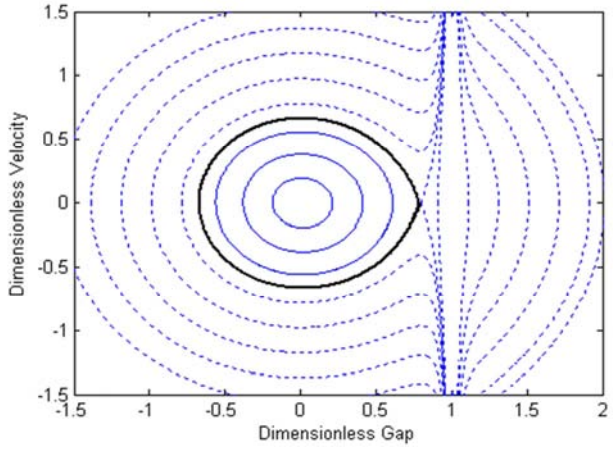

Figure 20. *Phase diagram for nano-beam with length 65 nm and given voltage 1 V.*

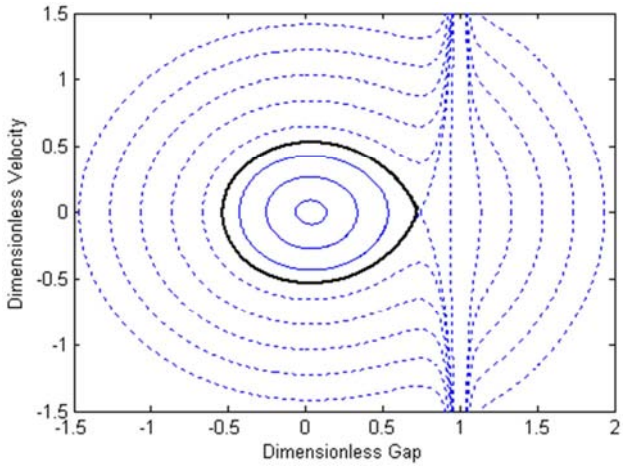

Figure 21. *Phase diagram for nano-beam with length 65 nm and given voltage 2 V.*

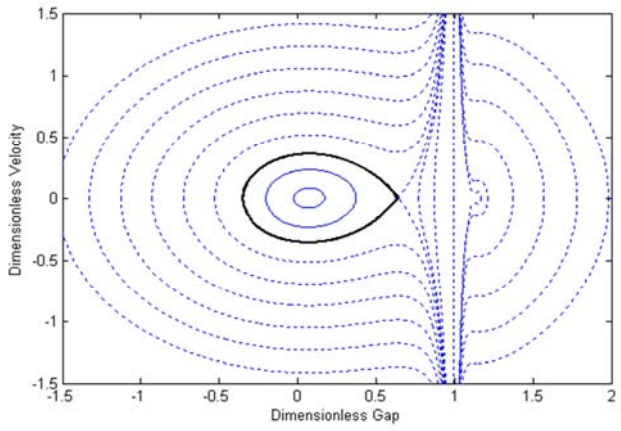

Figure 22. *Phase diagram for nano-beam with length 65 nm and given voltage 2.92 V.*

As mentioned a saddle type fixed point appearing in the beneath of the substrate, depends on the value of applied voltage and the length of the nano-beam. Since this saddle type fixed point is so close to the substrate position, a detailed view of motion trajectories is shown in Figs. 23. b and 24. b.

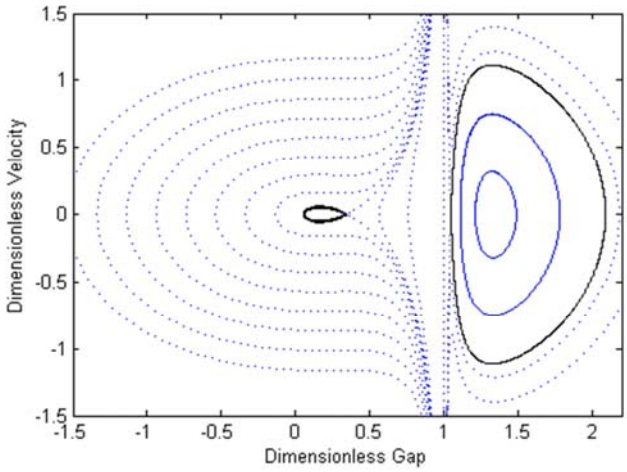

Figure 23a. *Phase diagram for the nano-beam with length 65 nm and given voltage 4 V.*

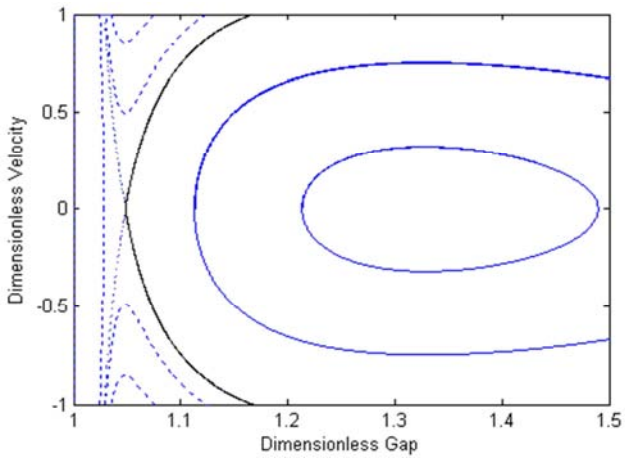

Figure 23b. *A detailed view of the phase diagram about the fixed points located under the substrate with length 65 nm and given voltage 4 V.*

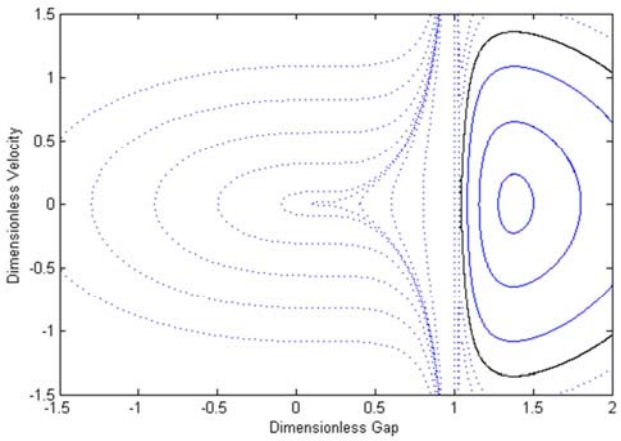

Figure 24a. *Phase diagram for nano-beam with length 65 nm and given voltage 4.5 V.*

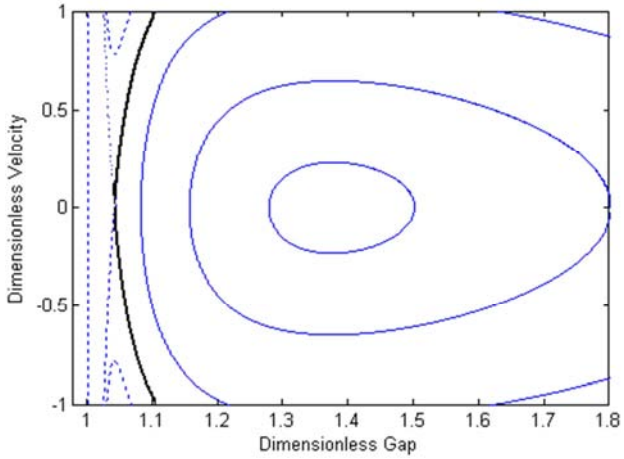

Figure 24b. *A detailed view of the phase diagram about the fixed points located under the substrate with length 65 nm and given voltage 4.5 V.*

For completeness purpose only, the bifurcation behavior of the nano-beam is also studied by neglecting VdW force. Figure 25 shows equilibrium points versus applied voltage for a nano-beam with considering only Casimir force and imposing electrostatic force. As shown in this figure the nano-beam has three fixed points in the range of $0 < V < V_{pull-in}$, which first and third points are stable center, and the second one is unstable saddle node. For the $V_{pull-in} < V$ the nano-beam has only one mathematically stable center point. As shown in this figure, saddle node bifurcation occurs in $V = V_{pull-in}$. Also, Figure 26 depicts motion trajectory of the nano-beam for input voltage *6V*.

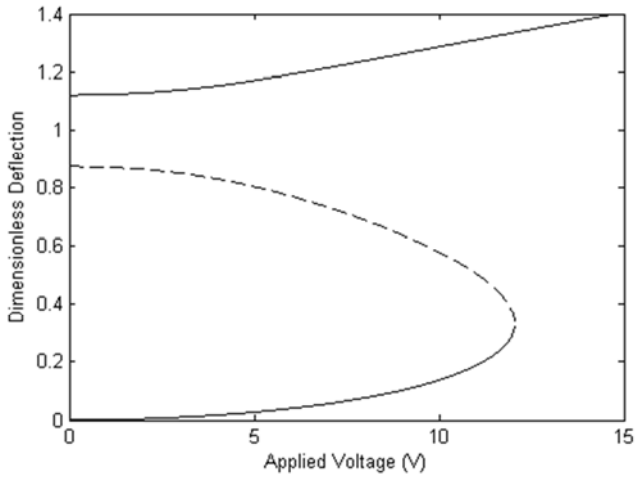

Figure 25. *Equilibrium points of a with given* $\gamma = 2.37\times10^{-4}$, $\alpha = 10^{-3}$ *and* $\beta = 0$ *model as* V *is varied.*

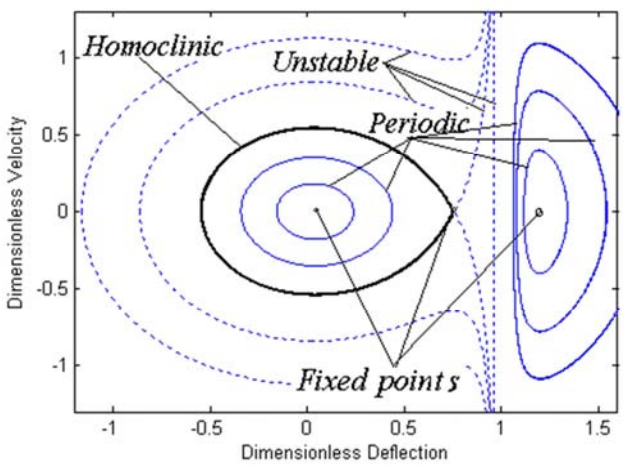

Figure 26. *Phase diagram with given* $\gamma = 2.37\times10^{-4}$, $\alpha = 10^{-3}$, $\beta = 0$ *and V=6V.*

4.4. Dynamic Response of Nano-Beam to Step DC Voltage

Dynamic response of the nano-beam system (nano switch) to a step DC voltage is numerically studied using Galerkin method [15]. For this cantilever nano-beam with *L=500nm, h=20nm, b=50nm, E=169GPa*, and $G_0 = 60nm$ the calculated dynamic pull-in voltage is V_{pullin}*=11.13* which is about 91.8% of the static pull-in voltages (Figure 12), indicating that the results are in good agreement with the reported works [28]. Figure 27 shows the time history of dimensionless deflection for this nano-beam with actuating step voltage of 11.12V. We note that the nano-beam oscillates with this applied voltage, and dose not collapse. As shown in Figure 28 by a small increase of the actuating step voltage by only about 0.01V the nano-beam collapses. Figure 28 shows the dynamic pull-in phenomenon (collapse point) with step DC voltages of 11.13V.

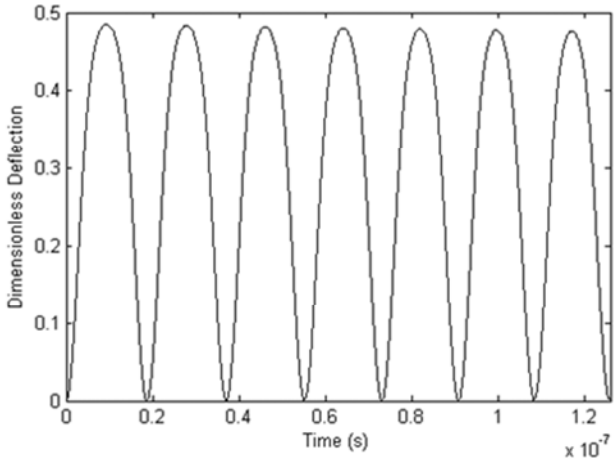

Figure 27. *Time history of nano-switch subjected to step-wise* $V_{DC} = 11.12$ *V.*

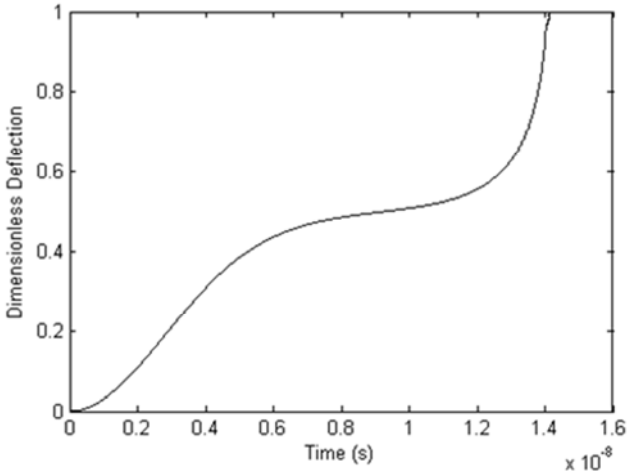

Figure 28. *Time history of nano-switch subjected to step-wise* $V_{DC} = 11.13$ *V.*

The phase portrait of the nano-beam with various step DC voltages is shown in Figure 29. This figure shows a metamorphosis of how a periodic orbit approaches homoclinic orbit at dynamic pull-in voltage. Indeed the periodic orbit is ended at dynamic pull-in voltage where a homoclinic orbit is formed. In another words when applied voltage approaches dynamic pull-in voltage the periods of the closed orbits tend to infinity. It can be said that there happens a homoclinic bifurcation [29] when the periodic orbit collides with a saddle point at dynamic pull-in voltage.

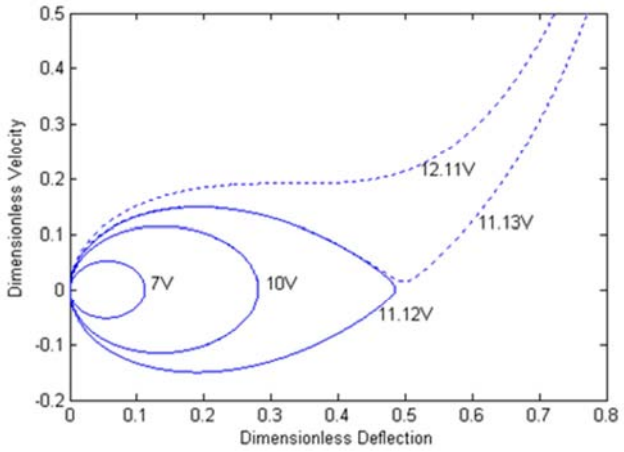

Figure 29. *Phase portrait of the nano-beam.*

5. Conclusion

In this article, Bifurcation behavior of a capacitive nano-beam was studied considering vdW and Casimir forces. A one degree of freedom mass-spring model was used and due to its low accuracy the elements of the model, considering static and dynamic behavior of the nano-beam in a distributed model, was adjusted using corrective coefficients. In order to determine values of the corrective coefficients, natural frequency, detachment parameter and static pull-in voltage of the nano-beam was obtained using distributed and mass-spring models, and then was equalized to each other. Solving equation of static deflection, fixed points or equilibrium position of the nano-beam is determined.

Results were showed that when the nano-beam is subjected to vdW and Casimir forces or only Casimir force, there exist three fixed points' in maximum, which first and third fixed points are stable center and second once is unstable saddle node. But when only vdW force was considered, it was showed that nano-beam has two equilibrium positions in maximum: the first is a stable center and the second is an unstable saddle node.

In all cases it was shown that, with increasing the nano-beam length as control parameter physically fixed points get near together and in a length well-known as detachment length they meet together by undergoing to a saddle node bifurcation.

Fixed points of nano-beam with imposing electrostatic force were obtained too. Results were showed that when vdW and Casimir forces or only Casimir force were considered, three fixed points appear in the range of $0 < V < V_{pull-in}$ which first and third ones are stable center and second once is an unstable saddle node. Furthermore it was shown that saddle node bifurcation occurs in $V = V_{pull-in}$.

When the nano-beam is subjected to vdW and electrostatic forces depends on the nano-beam length and the applied voltage an extra fixed point can be founded in the beneath of the substrate, which physically are impractical. With increasing the applied voltage as control parameter the fixed points located in the upper side of the nano-beam approach together and in a voltage well-known as pull-in voltage they meet together by undergoing to a saddle node bifurcation and the basin of attraction in phase plane in the upper side of the nano-beam disappears.

The dynamic response and the dynamic pull-in phenomena of the nano-beam have been obtained. The results showed that by increasing the value of the step-wise DC voltage to a critical value or dynamic pull-in voltage, the nano-beam goes to an unstable condition through a homoclinic bifurcation. It has also shown that the dynamic pull-in voltage at the presence of Casimir and vdW forces is about 91.8 % of the static pull-in voltage. The obtained results can be useful for NEMS community in behavioral studying of NEMS structures.

References

[1] P. Kim, C. M. Lieber, Nanotube nanotweezers, science. 286 (1999) 2148-2150.

[2] G-W. Wang, Y. Zhang, Y.-P. Zhao, G. T. Yang, Pull-in instability study of carbon nanotube tweezers under the influence of van der Waals force, Journal of Micromechanics and Microengineering. 14 (2004) 1119-1125.

[3] C. K. W. Adu, G. U. Sumanasekera, B. K. Pradhan, H. E. Romero, P. C. Eklund, Carbon nanotubes: a thermoelectric nano-nose, Chem. Phys. Lett. 337 (2001) 31-35.

[4] P. G. Collins, K. B. Bradley, M. Ishigami, A. Zettl, Extreme oxygen sensitivity of electronic properties of carbon nanotubes, Science. 287 (2000) 1801-1804.

[5] J. Arcamone, G. Rius, G. Abadal, J. Teva, N. Barnoli, F. Perez-Murano, Micro/nanomechanical resonators for distributed mass sensing with capacitive detection, Microelectronic Engineering. 83 (2006) 1216-1220.

[6] M. Dequesnes, Z. Tang, N. R. Aluru, Static and Dynamic Analysis of Carbon Nanotube-Based Switches, Journal of Engineering Materials and Technology. 126 (2004) 230-237.

[7] C.-H. Ke, N. Pugno, B. Peng, H. D. Espinosa, Experiments and modeling of carbon nanotube-based NEMS devices, Journal of the Mechanics and Physics of solids. 53 (2005) 1314-1333.

[8] T. Rueckes, K. Kim, E. Joselevich, G. Y. Tseng, C. L. Cheung, C. M. Lieber, Carbon nanotube-based nonvolatile random access memory for molecular computing, science. 289 (2000) 94-97.

[9] C. Li, E. T. Thostenson, T-W. Chou, Sensors and actuators based on carbon nanotubes and their composites: A review, Composites and Science and Technology. 68 (2008) 1227-1249.

[10] S. Senturia, Microsystem Design. Kluwer. Norwell. MA. USA; (2001).

[11] Y. Zhang, Y. P. Zhao, Numerical and analytical study on the pull-in instability of micro- structure under electrostatic loading, J Sens Actuators A Phys. 127 (2006) 366-367.

[12] H. B. G. Casimir On the attraction between two perfectly conducting plates. Proc K Ned Akad Wet. 51 (1948) 793–6.

[13] W. H. Lin, Y. P. Zhao, Nonlinear behavior for nanoscale electrostatic actuators with Casimir force, Chaos, Solitons and Fractals. 23 (2005) 1777-1785.

[14] E. M. Lifshitz, Sov. Phys. JETP, 2, 73 (1956).

[15] F. Vakili-Tahami, H. Mobki, A-A. keyvani-janbahan, G., Rezazadeh, Pull-in Phenomena and Dynamic Response of Capacitive Nano-beam Switch, sensors and transducers journal. 110 (2009) 26-37.

[16] W. H. Lin, Y. P. Zhao, Dynamic behavior of Nanoscale Electrostatic actuators, CHIN. PHYS. LETT. 20 (2003) 2070-2073.

[17] Azizi, A., H. Mobki, and G. Rezazadeh. "Bifurcation Behavior of a Capacitive Micro-Beam Suspended between Two Conductive Plates." Int J Sens Netw Data Commun 5. 149 (2016): 1-10.

[18] H. Mobki, M. H. Sadeghi, G. Rezazadeh, Design of Direct Exponential Observers for Fault Detection of Nonlinear MEMS Tunable Capacitor, IJE TRANSACTIONS A: Basics Vol. 28, No. 4, (2015) 634-641.

[19] H. Mobki, G. Rezazadeh, M. Sadeghi, F. Vakili-Tahami, M.-M. Seyyed-Fakhrabadi, A comprehensive study of stability in an electro-statically actuated micro-beam, International Journal of Non-Linear Mechanics. 48 (2013) 78-85.

[20] H. Mobki, M. H. Sadeghi, G. Rezazadeh, State Estimation of MEMs Capacitor Using Taylor Expansion, IJE TRANSACTIONS B: Applications Vol. 28, No. 5, (2015) 764-770.

[21] Fathi N. Mayoof, Muhammad A. Hawwa, Chaotic behavior of a curved carbon nanotube under harmonic excitation, Chaos, Solitons & Fractals, Volume 42, Issue 3, 2009, Pages 1860-1867.

[22] W. H. Lin, Y.-P. Zhao, Casimir effect on the pull-in parameters of nanometer switches, Microsystem Technologies. 11 (2005) 80-85.

[23] W.-H. Lin, Y.-P., Zhao, Stability and bifurcation behavior of electrostatic torsional NEMS varactor influence by dispersion forces, Journal of Physics D: Applied Physics. 40 (2007) 1649-1654.

[24] Zarei, O., Rezazadeh, G., [2008] "A Novel Approach to Study of Mechanical Behavior of NEM Actuators Using Galerkin Method", International Journal of Nanosystems 1 (2), pp. 161-169.

[25] J. D. Jackson, Classical Electrodynamics, 3rd Ed, Wiley, New York (1998).

[26] J. N. Israelachvili, Intermolecular and surface forces, Academic, London (1992).

[27] J. G. Guo, Y. P. Zhao, Influence of van der Waals and Casimir Force on Electrostatic Tensional Actuators, microelectromechanical systems. 13 (2004) 1027-1035.

[28] G. K. Ananthasuresh, R. K. Gupta, S. D. Senturia, An approach to macromodeling of MEMS for nonlinear dynamic simulation, In Proceedings of the ASME International Conference of Mechanical Engineering Congress and Exposition (MEMS), Atlanta, GA (1996) 401–407.

[29] Y. A. Kuznetsov, Elements of Applied Bifurcation Theory. Second Edition, Springer-Verlag, New York (1997).